Research Square

Preprints are preliminary reports that have not undergone peer review.
They should not be considered conclusive, used to inform clinical practice,
or referenced by the media as validated information.

Evaluation of robustness of optimization methods in breast intensity-modulated radiation therapy using TomoTherapy

Yuya Oki (yuya.oki1002@gmail.com)
Kobe Minimally Invasive Cancer Center https://orcid.org/0000-0002-9145-255X
Hiroaki Akasaka
Kobe Minimally Invasive Cancer Center
Kazuyuki Uehara
Kobe Minimally Invasive Cancer Center
Kazufusa Mizonobe
Kobe Minimally Invasive Cancer Center
Masanobu Sawada
Kobe Minimally Invasive Cancer Center
Junya Nagata
Kobe Minimally Invasive Cancer Center
Aya Harada
Kobe Minimally Invasive Cancer Center
Hiroshi Mayahara
Kobe Minimally Invasive Cancer Center

Research Article

Keywords: breast cancer, intensity-modulated radiation therapy, TomoTherapy, robust planning, virtual bolus, skin flash

Posted Date: June 23rd, 2022

DOI: https://doi.org/10.21203/rs.3.rs-1628398/v1

License: This work is licensed under a Creative Commons Attribution 4.0 International License.
Read Full License

Version of Record: A version of this preprint was published at Physical and Engineering Sciences in Medicine on January 24th, 2024. See the published version at https://doi.org/10.1007/s13246-023-01377-7.

Abstract

Introduction: Intensity-modulated radiation therapy (IMRT) has become a popular choice for breast cancer treatment. We aimed to evaluate and compare the robustness of each optimization method used for breast IMRT using TomoTherapy.

Methods: A retrospective analysis was performed on 10 patients with left breast cancer. For each optimization method (clipping, virtual bolus, and skin flash), a corresponding 50 Gy/25 fr plan was created in the helical and direct TomoTherapy modes. The dose-volume histogram parameters were compared after shifting the patients anteriorly and posteriorly.

Results: In the helical mode, when the patient was not shifted, the median D1cc (minimum dose delivered to 1 cc of the organ volume) for breast skin for the clipping and virtual bolus plans were 52.2 (interquartile range: 51.9–52.6) and 50.4 (50.1–50.8) Gy, respectively. After an anterior shift, the D1cc of the breast skin for the clipping and virtual bolus plans was 56.0 (55.6–56.8) and 50.9 (50.5–51.3) Gy, respectively. When the direct mode was used without shifting the patient, the D1cc of the breast skin for the clipping, virtual bolus, and skin flash plans were 52.6 (51.9–53.1), 53.4 (52.6–53.9), and 52.3 (51.7–53.0) Gy, respectively. After shifting anteriorly, D1cc of the breast skin for the clipping, virtual bolus, and skin flash plans was 55.6 (54.1–56.4), 52.4 (52.0–53.0), and 53.6 (52.6–54.6) Gy, respectively.

Conclusions: The clipping method is not sufficient for breast IMRT. The virtual bolus and skin flash methods were more effective optimization methods according to our analyses.

Introduction

Radiation therapy is commonly employed to treat breast cancer [1, 2], and three-dimensional conformal radiotherapy (3D-CRT) with tangential beams is the method used most often. In recent years, intensity-modulated radiation therapy (IMRT) and volumetric modulation arc therapy (VMAT) have gained popularity because of their abilities to reduce radiation doses reaching the heart and ipsilateral lung during breast irradiation [3-12].

When inverse planning is performed on a superficial target, fluence of the tangential beam may increase near the skin surface to compensate for a lack of build-up material [13, 14]. To avoid this, target clipping or the virtual bolus technique is used during IMRT optimization for superficial targets [15]. The target clipping technique is a simple method, which is used universally for head and neck IMRT [16, 17]. During target clipping, the target is trimmed so as to maintain a specific distance between the surface of the skin and the target. For example, Ashburner et al. recommend the target be clipped to maintain a 3-mm gap between the target and skin surface [15]. In contrast, the virtual bolus is only used for optimization, and the bolus is removed in the final calculations. Fluence boosting in the build-up region can be suppressed using the virtual bolus method in TomoTherapy [18-20]. Although target clipping and virtual bolus plans are available for superficial targets, breast IMRT may have a larger beamlet-boosting effect because of the frequent use of tangential beams.

During 3D-CRT planning, the skin flash technique is often used for breast radiation therapy. Skin flash involves opening additional multi-leaf collimator (MLC) leaves to the outside of the treatment volume as a means of compensating for setup error and respiratory motion. Although skin flash cannot be used in helical TomoTherapy, in which rotational beam delivery is employed, it can be used for TomoDirect, in which beam delivery occurs at a fixed gantry angle. TomoDirect is advantageous for breast radiation therapy because the low-dose spread to the lungs is reduced [21, 22]. Kang et al. reported that skin flash maintains coverage of the target in TomoDirect plans when a setup error occurs [23].

Overall, various optimization methods for breast IMRT exist. However, to the best of our knowledge, there have been no studies evaluating the robustness of each optimization technique using TomoTherapy. Thus, the purpose of this study was to investigate the efficacy of each optimization method considering changes to patient positioning (i.e., setup error or respiratory motion) that may occur in treatment situations. The investigations in this study focused on the dose uncertainty at the breast surface.

Methods

A. Patient selection and contouring

A retrospective study was performed involving 10 patients who received radiation therapy after breast-conserving surgery for left breast cancer. This study was approved by our institutional ethics committee. Plans were generated for patients who were treated in our hospital between April 2019 and March 2022. The median age of the patients was 59 years (range: 38–82). The TMN classification of the patients were as follows: T0N1M0 (n = 1), T0N1M0 (n =1), T1N2M0 (n = 1), T1N2M0 (n = 1), T2N1M0 (n = 2), T2N2M0 (n = 1), T3N2M0 (n = 1), T4bN1M0 (n = 1), T4bN3M0 (n = 1).

Computed tomography (CT, Aquilion64, Canon Medical Systems, Tochigi, Japan) scans were acquired with a 2-mm slice thickness, head-first supine position, and free breathing mode. Patients were immobilized using the VacLok system (CIVCO Medical Solutions, Kalona, IA) with the use of a wing board for arm positioning above the head. The CT data were imported into Velocity, version 4.0.1 (Varian Medical Systems, Palo Alto, CA, USA) and used to create a structure set. The clinical target volume (CTV) included the left breast and the axillary and supraclavicular lymph node areas. The planning target volume (PTV) was defined as the CTV with a 5-mm margin in all directions. The ipsilateral lung, contralateral lung, heart, contralateral breast, spinal cord, esophagus, stomach, thyroid gland, and larynx were contoured as organs at risk.

For evaluation, breast skin was defined as the area of the left breast within 5 mm of the skin surface (Fig. 1a). The clipping target was defined as the area where the PTV intersects the area of the body contour reduced inward by 3 mm. (Fig. 1b). The virtual bolus was created by expanding the PTV to 5 mm and subtracting the body contour. The density of the virtual bolus was then replaced by 1.0 g/cm^3 in the TomoTherapy planning system (Fig. 1c). The virtual bolus was only used during optimization, and the final calculation was performed without the virtual bolus.

B. Treatment planning

Plans were created for the TomoHD system, version 2.1.6 (Accuray Inc., Sunnyvale, CA, USA), which has a 6 MV photon beam with a dose rate of 850 MU/min modulated with 64 binary MLC. The plans were generated in Planning Station, version 5.1.1.6 (Accuray Inc.) with a collapsed cone convolution/superposition algorithm. Dose constraints are shown in Table 1. For the virtual bolus plans, the prescribed dose was 50 Gy to 50% (D50) of the PTV and was delivered in 25 fractions. For the clipping and skin flash plans, a prescription point was set at D50 of the clipped PTV. The plan parameters included a fixed jaw of 2.5 cm, modulation factor of 2.0–2.3, and calculation grid of 1.91 × 1.91 × 2 mm^3. In helical mode, a pitch of 0.287 was used, and a directional block (with only beam ejection allowed) was set on part of the bilateral lungs. In direct mode, the pitch was set to 0.250, and the beam angle was tangential to the breast, while two oblique beam angles were used for the lymph node area. When using skin flash, the target was clipped 3 mm from the skin surface, and the outer three MLC leaves (1.875 cm width) were extended (Fig. 1d).

C. Plan evaluation

TomoTherapy DQA Station version 5.1.1.5 (Accuray Inc.) was used to simulate how patient position variation impacted the delivered dose. To simulate setup error, recalculations were performed with the patients positioned at the origin (no shift) and then with the patients being displaced in the anterior or posterior directions. The DICOM-RT files of the recalculated plans were exported, and the dose-volume histograms (DVH) were analyzed using Velocity. Moreover, to compare the dose distributions and profiles between the plans when shifted 5 mm in the anterior/posterior direction and the origin position, an analysis was performed using in-house software based on Python (version 3.8.10) with NumPy (version 1.21.4), Pydicom (version 2.2.2), and Matplotlib (version 3.5.1) modules.

D. Statistical analysis

Data are presented as median ± interquartile range (IQR). All statistical analyses were performed using R, version 4.0.2 (R Foundation for Statistical Computing) [24]. The differences between the two groups were analyzed using Wilcoxon signed rank test. For three groups comparisons, the Friedman test followed by pairwise post hoc comparisons using the Wilcoxon signed rank test with Bonferroni corrections were used. Data were considered statistically significant if $p < 0.05$.

Results

A. DVH parameters

The DVH parameters for helical mode and direct mode are shown in Table 2(a) and (b), respectively. With respect to the helical mode, there was no significant difference in D98 for the CTV after the anterior shift. However, the clipping plans showed a significant increase in D2 of the CTV and D1cc of the breast skin. The median D1cc of the breast skin for the clipping plans was 56.0 Gy, exceeding 110% of the prescribed

dose. In contrast, the virtual bolus plan showed no significant difference in D1cc of the breast skin. On the other hand, after shifting posteriorly, D98 of the CTV was significantly reduced for both optimization methods, whereas D98 of the breast skin was significantly reduced only in the clipping plan. The D2 of the CTV increased significantly for both optimization methods.

With respect to the direct mode, as with the helical mode, there was no significant difference in D98 for the CTV and the breast skin after shifting anteriorly. However, the clipping plans showed a significant increase in D2 for the CTV and D1cc for the breast skin. The median value of D1cc of the breast skin for the clipping plans was 55.6 Gy, exceeding 110% of the prescribed dose. The skin flash plans also significantly increased D1cc for the breast skin, but within 110% of the prescribed dose in most cases, which is clinically acceptable. Conversely, after posteriorly shifting, all plans showed a significant decrease in D98 and a significant increase in D2 for the CTV. D98 of the breast skin was significantly reduced in all optimization methods, while D1cc was not significantly changed exclusively in the virtual bolus plan.

B. Difference in DVH parameters compared to origin position

To examine the differences between the optimization techniques, the differences in DVH parameters between the origin position and the anterior/posterior shifted plans are shown in Table 3. For the helical mode (Table 3a), after shifting anteriorly, the DD1cc of the breast skin and D2 of the CTV for the clipping plans were significantly worse than the virtual bolus plans. In contrast, after posteriorly shifting, the difference relative to the origin position was small regardless of the optimization method.

When using the direct mode (Table 3b), after the patient was shifted anteriorly, DD1cc for the breast skin was significantly worse for the clipping plans compared to the other two methods. There was no notable difference between the virtual bolus plans and the skin flash plans. After the patient was shifted posteriorly, there was no significant difference in DD98 and DD1cc of the breast skin.

C. Dose distribution / profile

The dose distributions and profiles for each plan using the helical mode are shown in Figure 2. After an anterior shift, focusing on the breast skin, hot spots occurred in the clipping plan. However, the virtual bolus plan showed little change in dose distribution. The dose profile showed a large increase in dose at the breast skin in the clipping plan. Conversely, after a posterior shift, there was little difference between each optimization method.

Similarly, the dose distributions and profiles of the direct mode are shown in Figure 3. After the anterior shift, hot spots were observed on the skin surface in the clipping plan. However, the virtual bolus and skin flash plans showed little change in dose on the breast skin. After the posterior shift, as in the helical mode, there was no notable difference between optimization methods. As for the dose profile, an increase in dose was noted on the breast skin in the clipping plan. In addition, the dose profiles showed that the

dose was approximately 2–3% higher in the virtual bolus plans than in the other plans, with or without shifts.

Discussion

In this study, the virtual bolus and skin flash methods were shown to be the most robust optimization techniques. MVCT imaging of TomoTherapy requires longer imaging times than kV imaging [25]. Therefore, there is uncertainty in positioning due to the respiratory motion of the chest wall. In addition, because of the longer irradiation time compared to VMAT, there are concerns about the effects of respiratory motion and baseline drift of breathing [26]. Thus, it is important to create plans that are robust with regard to setup errors.

Although the clipping method is commonly used for superficial targets, as is done in head and neck IMRT [16, 17], the results of this study indicate that the clipping technique is less robust for breast IMRT. In superficial targets, the tangential fluence increases because of a lack of build-up material. A plan that provides excessive fluence to the skin may have a lower objective function [13, 14]. In breast IMRT, the beam weights in the tangential direction are high to avoid irradiation to the heart and ipsilateral lung. Therefore, the fluence-boosting effects are expected to be greater. As a result, even when the clipping method was applied, it was considered insufficient to compensate for the lack of build-up material. In addition, ΔD98 of breast skin tended to be decreased in the clipping plan than in the other plans (Table 3). It should also be noted that in the case of breast IMRT, the use of the clipping method results in a steeper dose fall-off at the breast skin, and it may result in an insufficient dose near the breast skin.

The use of a virtual bolus can prevent hotspots on the skin surface during total body and total scalp irradiation using TomoTherapy [18–20]. It has been reported that a virtual bolus of the PTV + 5-mm thickness was effective in total scalp irradiation using helical TomoTherapy, which mainly uses tangential beams as is used during breast irradiation [20]. In this study, the virtual bolus of the PTV + 5-mm thickness was demonstrated to be useful in breast IMRT using TomoTherapy. However, in some patients, the D1cc of the breast skin exceeded 110% of the prescribed dose when setup error occurred in the posterior direction in direct mode (Table 2b). Moreover, the dose profiles of virtual bolus plans are higher than those of the other two methods (Fig. 3b). The reason is that the direct mode, which uses only tangential beams, is more strongly impacted because of the change in target depth caused by the virtual bolus. Currently, TomoTherapy treatment planning systems do not provide a dose normalization function; therefore, the skin flash method would be a better option for this problem. In addition, the virtual bolus plan showed a tendency for D98 of the breast skin to be lower than other optimization methods at the origin position (Table 2a). Therefore, if irradiation of the skin surface is necessary, a real bolus is typically recommended [27, 28]. Furthermore, Sakai et al. reported that an immobilizing thermoplastic shell can substitute a bolus [28]. In addition to compensating for the lack of build-up material, this substitution would reduce the uncertainty caused by respiratory motion, which would also be effective in enhancing robustness.

For the skin flash method, it was confirmed that the method can be used to create a plan that is robust against setup error. Currently, there are few reports on the robustness of the skin flash method in TomoTherapy. When skin flash is used in direct mode, the fluence of the additional MLC leaves is determined by the average intensity of the second and third leaves from the outside of the beam edge. Therefore, excessive fluence to the skin did not occur because there was sufficient build-up material, and no hotspots were observed when the patients were shifted in the anterior direction. However, the beamlet-boosting effect may occur if the target contains low-density regions, such as air outside the body or in the lungs. Therefore, it should be noted that optimization must be performed for clipped targets when skin flash is used in TomoTherapy.

In recent years, performing breast radiation therapy over a shorter treatment period has become a standard practice [2, 29–30]. Considering this, the impact of setup error in a single fraction has increased. Therefore, the robustness of each plan must be independently considered. Another method for maximizing robustness is to use an optimization technique with a model of probability density functions that describe the breathing motion [31–33]. However, treatment planning systems utilizing such an approach are limited and have not been universally adopted. Based on the results of this study, it was recommended that the virtual bolus and skin flash methods be applied in breast IMRT. In addition, it was suggested that the clipping method is less robust than these two methods.

The results of this study are limited because the patient is simply moved to the anterior or posterior direction to evaluate robustness. In practice, organ deformation due to breathing should also be considered. Further investigations should be conducted using expiratory/inspiratory CT or 4DCT to account for actual respiratory motion.

Conclusion

For breast IMRT, the most robust optimization methods include the use of a virtual bolus and skin flash. Our results suggest that the clipping method, which is commonly used for superficial targets, may be unsuitable for breast IMRT.

Declarations

Acknowledgements

We would like to thank Editage (www.editage.com) for the English language editing of this manuscript.

Funding

This research did not receive any specific grant from funding agencies in the public, commercial, or not-for-profit sectors.

Competing Interests

The authors have no relevant financial or non-financial interests to disclose.

Ethics Approval

This study was performed in line with the principles of the Declaration of Helsinki. Approval was granted by the Ethics Committee of our institution (No: 2021-kenkyu03-13).

Consent to participate

Informed consent was obtained from all individual participants included in the study.

Consent to publish

The authors affirm that all participants provided informed consent for publication of the images in Figure 1, 2 and 3.

Data Availability Statement

Research data are stored in an institutional repository and will be shared upon request to the corresponding author.

Author Contributions

YO, HA, KU, KM, AH and HM made substantial contributions to the study design and data interpretation. YO, MS and JN made substantial contributions to data acquisition and analysis. All authors critically revised the report for important intellectual content, commented on drafts of the manuscript, and approved the final version of the report. All authors agree to be accountable for all aspects of the work and ensuring that questions related to the accuracy or integrity of any part of the report are appropriately investigated and resolved.

References

1. Pan HY, Haffty BG, Falit BP, Buchholz TA, Wilson LD, Hahn SM, Smith BD (2016) Supply and demand for radiation oncology in the United States: updated projections for 2015 to 2025. Int J Radiat Oncol Biol Phys 96:493–500. https://doi.org/10.1016/j.ijrobp.2016.02.064
2. Smith BD, Bellon JR, Blitzblau R, Freedman G, Haffty B, Hahn C, Halberg F, Hoffman K, Horst K, Moran J, Patton C, Perlmutter J, Warren L, Whelan T, Wright JL, Jagsi R (2018) Radiation therapy for the whole breast: executive summary of an American Society for Radiation Oncology (Astro) evidence-based guideline. Pract Radiat Oncol 8:145–152. https://doi.org/10.1016/j.prro.2018.01.012
3. Beckham WA, Popescu CC, Patenaude VV, Wai ES, Olivotto IA (2007) Is multibeam IMRT better than standard treatment for patients with left-sided breast cancer? Int J Radiat Oncol Biol Phys 69:918–924. https://doi.org/10.1016/j.ijrobp.2007.06.060

4. Michalski A, Atyeo J, Cox J, Rinks M, Morgia M, Lamoury G (2014) A dosimetric comparison of 3D-CRT, IMRT, and static tomotherapy with an SIB for large and small breast volumes. Med Dosim 39:163–168. https://doi.org/10.1016/j.meddos.2013.12.003
5. Rudat V, Alaradi AA, Mohamed A, Ai-Yahya K, Altuwaijri S (2011) Tangential beam IMRT versus tangential beam 3D-CRT of the chest wall in postmastectomy breast cancer patients: a dosimetric comparison. Radiat Oncol 6:26. https://doi.org/10.1186/1748-717X-6-26
6. Bogue J, Wan J, Lavey RS, Parsai EI (2019) Dosimetric comparison of VMAT with integrated skin flash to 3D field-in-field tangents for left breast irradiation. J Appl Clin Med Phys 20:24–29. https://doi.org/10.1002/acm2.12527
7. Huang JH, Wu XX, Lin X, Shi JT, Ma YJ, Duan S, Huang XB (2019) Evaluation of fixed-jaw IMRT and tangential partial-VMAT radiotherapy plans for synchronous bilateral breast cancer irradiation based on a dosimetric study. J Appl Clin Med Phys 20:31–41. https://doi.org/10.1002/acm2.12688
8. Rossi M, Virén T, Heikkilä J, Seppälä J, Boman E (2021) The robustness of VMAT radiotherapy for breast cancer with tissue deformations. Med Dosim 46:86–93. https://doi.org/10.1016/j.meddos.2020.09.005
9. Borca VC, Franco P, Catuzzo P, Migliaccio F, Zenone F, Aimonetto S, Peruzzo A, Pasquino M, Russo G, La Porta MR, Cante D, Sciacero P, Girelli G, Ricardi U, Tofani S (2012) Does TomoDirect 3DCRT represent a suitable option for post-operative whole breast irradiation? A hypothesis-generating pilot study. Radiat Oncol 7:211. https://doi.org/10.1186/1748-717X-7-211
10. Mast ME, van Kempen-Harteveld L, Heijenbrok MW, Kalidien Y, Rozema H, Jansen WP, Petoukhova AL, Struikmans H (2013) Left-sided breast cancer radiotherapy with and without breath-hold: does IMRT reduce the cardiac dose even further? Radiother Oncol 108:248–253. https://doi.org/10.1016/j.radonc.2013.07.017
11. Jagsi R, Griffith KA, Moran JM, Ficaro E, Marsh R, Dess RT, Chung E, Liss AL, Hayman JA, Mayo CS, Flaherty K, Corbett J, Pierce L (2018) A randomized comparison of radiation therapy techniques in the management of node-positive breast cancer: primary outcomes analysis. Int J Radiat Oncol Biol Phys 101:1149–1158. https://doi.org/10.1016/j.ijrobp.2018.04.075
12. Jin GH, Chen LX, Deng XW, Liu XW, Huang Y, Huang XB (2013) A comparative dosimetric study for treating left-sided breast cancer for small breast size using five different radiotherapy techniques: conventional tangential field, filed-in-filed, tangential-IMRT, multi-beam IMRT and VMAT. Radiat Oncol 8:89. https://doi.org/10.1186/1748-717X-8-89
13. Thomas SJ, Hoole ACF (2004) The effect of optimization on surface dose in intensity modulated radiotherapy (IMRT). Phys Med Biol 49:4919–4928. https://doi.org/10.1088/0031-9155/49/21/005
14. Nguyen TB, Hoole ACF, Burnet NG, Thomas SJ (2009) The optimization of intensity modulated radiotherapy in cases where the planning target volume extends into the build-up region. Phys Med Biol 54:2511–2525. https://doi.org/10.1088/0031-9155/54/8/017
15. Ashburner MJ, Tudor S (2014) The optimization of superficial planning target volumes (PTVs) with helical tomotherapy. J Appl Clin Med Phys 15:4560. https://doi.org/10.1120/jacmp.v15i6.4560

16. Franceschini D, Paiar F, Meattini I, Agresti B, Pasquetti EM, Greto D, Bonomo P, Marrazzo L, Casati M, Livi L, Biti G (2013) Simultaneous integrated boost-intensity-modulated radiotherapy in head and neck cancer. Laryngoscope 123:E97–E103. https://doi.org/10.1002/lary.24257
17. Johnston M, Guo L, Back M, Guminski A, Lee A, Hanna C, Veivers D, Wignall A, Eade T (2013) Intensity-modulated radiotherapy using simultaneous-integrated boost for definitive treatment of locally advanced mucosal head and neck cancer: outcomes from a single-institution series. J Med Imaging Radiat Oncol 57:356–363. https://doi.org/10.1111/1754-9485.12033
18. Moliner G, Izar F, Ferrand R, Bardies M, Ken S, Simon L (2015) Virtual bolus for total body irradiation treated with helical tomotherapy. J Appl Clin Med Phys 16:164–176. https://doi.org/10.1120/jacmp.v16i6.5580
19. Lobb E (2014) Bolus-dependent dosimetric effect of positioning errors for tangential scalp radiotherapy with helical tomotherapy. Med Dosim 39:93–97. https://doi.org/10.1016/j.meddos.2013.10.005
20. Takenaka R, Haga A, Nawa K, Hideomi Y, Nakagawa K (2019) Improvement of the robustness to set up error by a virtual bolus in total scalp irradiation with Helical TomoTherapy. Radiol Phys Technol 12:433–437. https://doi.org/10.1007/s12194-019-00539-1
21. Tang D, Liang Z, Guan F, Yang Z (2020) Dosimetric and radiobiological comparison of five techniques for postmastectomy radiotherapy with simultaneous integrated boost. BioMed Res Int 2020:9097352. https://doi.org/10.1155/2020/9097352
22. Takano S, Omura M, Suzuki R, Tayama Y, Matsui K, Hashimoto H, Hongo H, Nagata H, Tanaka K, Hata M, Inoue T (2019) Intensity-modulated radiation therapy using TomoDirect for postoperative radiation of left-sided breast cancer including lymph node area: comparison with TomoHelical and three-dimensional conformal radiation therapy. J Radiat Res 60:694–704. https://doi.org/10.1093/jrr/rrz052
23. Kang DG, Park SI, Kim SH, Chung MJ, Lee KM, Lee JH (2015) Evaluation of the Flash effect in breast irradiation using TomoDirect: an investigational study. J Radiat Res 56:397–404. https://doi.org/10.1093/jrr/rru118
24. R Core Team (2020) R: A Language and Environment for Statistical Computing. R Foundation for Statistical Computing
25. Takahashi Y, Vagge S, Agostinelli S, Han E, Matulewicz L, Schubert K, Chityala R, Ratanatharathorn V, Tournel K, Penagaricano JA, Florian S, Mahe MA, Verneris MR, Weisdorf DJ, Corvo R, Dusenbery KE, Storme G, Hui SK (2015) Multi-institutional feasibility study of a fast patient localization method in total marrow irradiation with helical tomotherapy: a global health initiative by the international consortium of total marrow irradiation. Int J Radiat Oncol Biol Phys 91:30–38. https://doi.org/10.1016/j.ijrobp.2014.09.014
26. Ricotti R, Ciardo D, Fattori G, Leonardi MC, Morra A, Dicuonzo S, Rojas DP, Pansini F, Cambria R, Cattani F, Gianoli C, Spinelli C, Riboldi M, Baroni G, Orecchia R, Jereczek-Fossa BA (2017) Intra-

fraction respiratory motion and baseline drift during breast Helical Tomotherapy. Radiother Oncol 122:79–86. https://doi.org/10.1016/j.radonc.2016.07.019

27. Akasaka H, Oki Y, Mizonobe K, Uehara K, Mayahara H, Harada A, Hashimoto N, Kitatani K, Yabuuchi T, Ishihara T, Iwashita K, Miyawaki D, Mukumoto N, Nakaoka A, Sasaki R (2021) The air gap between bolus and skin affects dose distribution in helical and direct tomotherapy. J Radiother Pract 20:294–299. https://doi.org/10.1017/S1460396920000333
28. Sakai Y, Tanooka M, Okada W, Sano K, Nakamura K, Shibata M, Ueda Y, Mizuno H, Tanaka M (2021) Characteristics of a bolus created using thermoplastic sheets for postmastectomy radiation therapy. Radiol Phys Technol 14:179–185. https://doi.org/10.1007/s12194-021-00618-2
29. Nozaki M, Kagami Y, Machida R, Nakamura K, Ito Y, Nishimura Y, Teshima T, Saito Y, Nagata Y, Matsumoto Y, Akimoto T, Hiraoka M, Japan Clinical Oncology Group, Radiation Therapy Study Group (2021) Final analysis of a Multicenter Single-Arm Confirmatory Trial of hypofractionated whole breast irradiation after breast-conserving surgery in Japan: JCOG0906. Jpn J Clin Oncol 51:865–872. https://doi.org/10.1093/jjco/hyab024
30. Murray Brunt A, Haviland JS, Wheatley DA, Sydenham MA, Alhasso A, Bloomfield DJ, Chan C, Churn M, Cleator S, Coles CE, Goodman A, Harnett A, Hopwood P, Kirby AM, Kirwan CC, Morris C, Nabi Z, Sawyer E, Somaiah N, Stones L, Syndikus I, Bliss JM, Yarnold JR, FAST-Forward Trial Management Group (2020) Hypofractionated breast radiotherapy for 1 week versus 3 weeks (FAST-Forward): 5-year efficacy and late normal tissue effects results from a multicentre, non-inferiority, randomised, phase 3 trial. Lancet 395:1613–1626. https://doi.org/10.1016/S0140-6736(20)30932-6
31. Bortfeld T, Chan TCY, Trofimov A, Tsitsiklis JN (2008) Robust management of motion uncertainty in intensity-modulated radiation therapy. Oper Res 56:1461–1473. https://doi.org/10.1287/opre.1070.0484
32. Chan TCY, Bortfeld T, Tsitsiklis JN (2006) A robust approach to IMRT optimization. Phys Med Biol 51:2567–2583. https://doi.org/10.1088/0031-9155/51/10/014
33. Byrne M, Hu Y, Archibald-Heeren B (2016) Evaluation of RayStation robust optimisation for superficial target coverage with setup variation in breast IMRT. Australas Phys Eng Sci Med 39:705–716. https://doi.org/10.1007/s13246-016-0466-6

Tables

Tables 1 to 3 are available in the Supplementary Files section

Figures

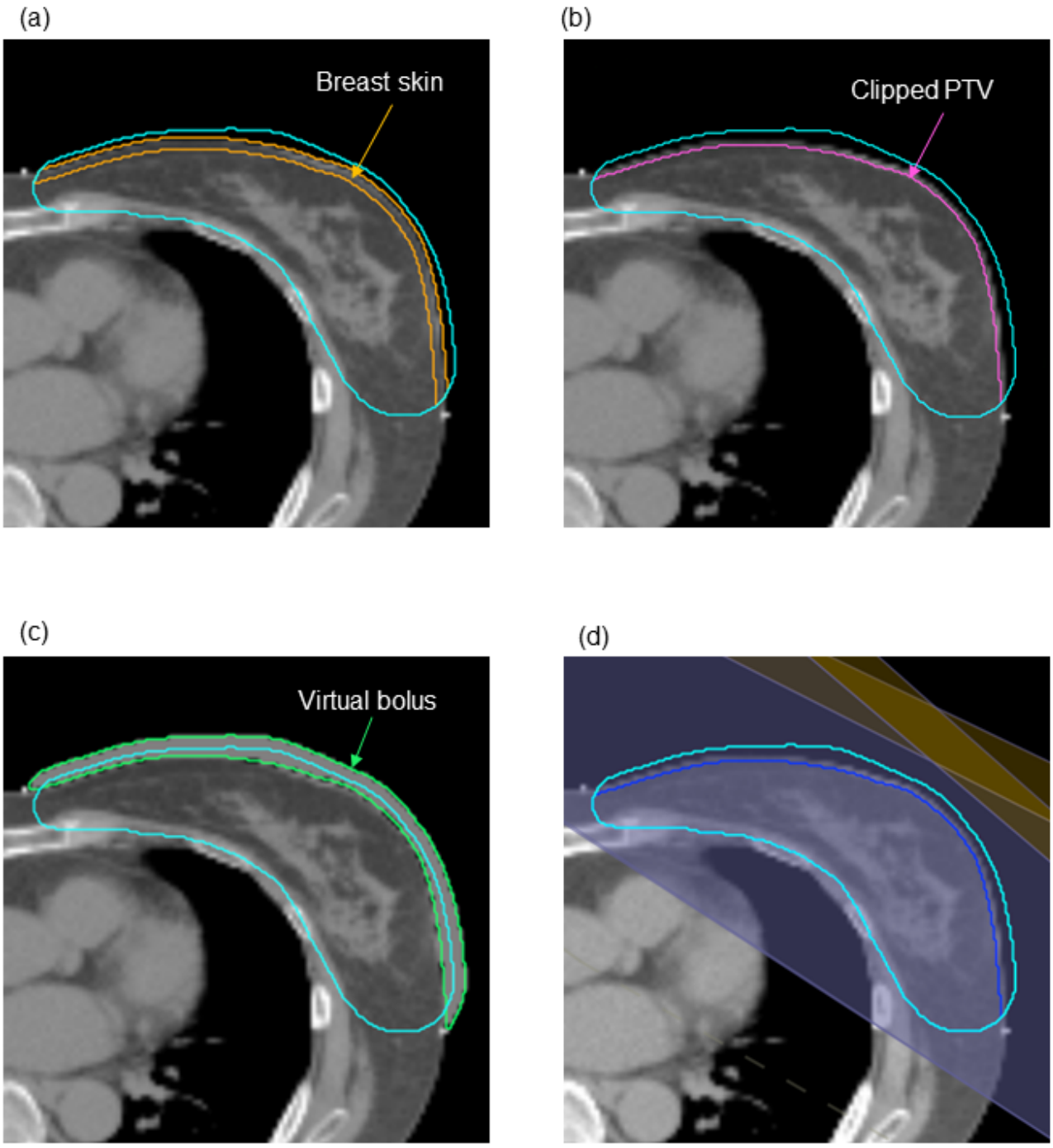

Figure 1

Contouring

(a) Contours of the planning target volume (PTV; cyan) and breast skin (yellow) in the axial plane; (b) 3 mm clipped PTV (pink); (c) virtual bolus of PTV + 5-mm thickness (green); and (d) beam angle of TomoDirect plans (blue band) and the skin flash area (yellow band)

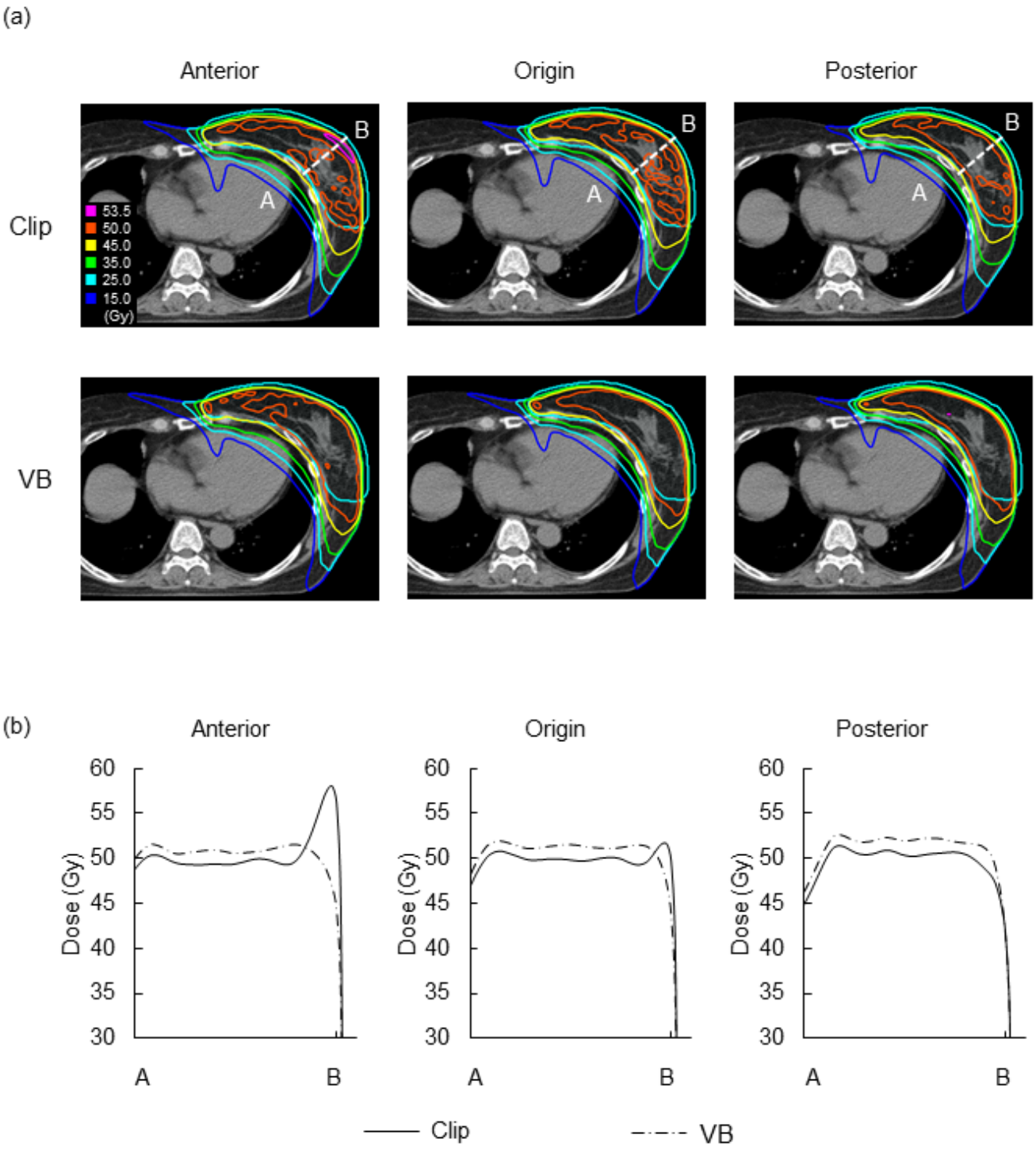

Figure 2

Dose distributions for plans used in helical mode

(a) From the left column, the following data are shown in helical mode: dose distribution after shifting in the anterior direction, the dose distribution at the origin position, and dose distribution after shifting in the posterior direction. Each row, from top to bottom, shows the clipping and virtual bolus plans. (b) Dose

profile along line AB for plans after shifting in the anterior direction, at the origin position, and after shifting posterior direction

Abbreviation: VB; virtual bolus

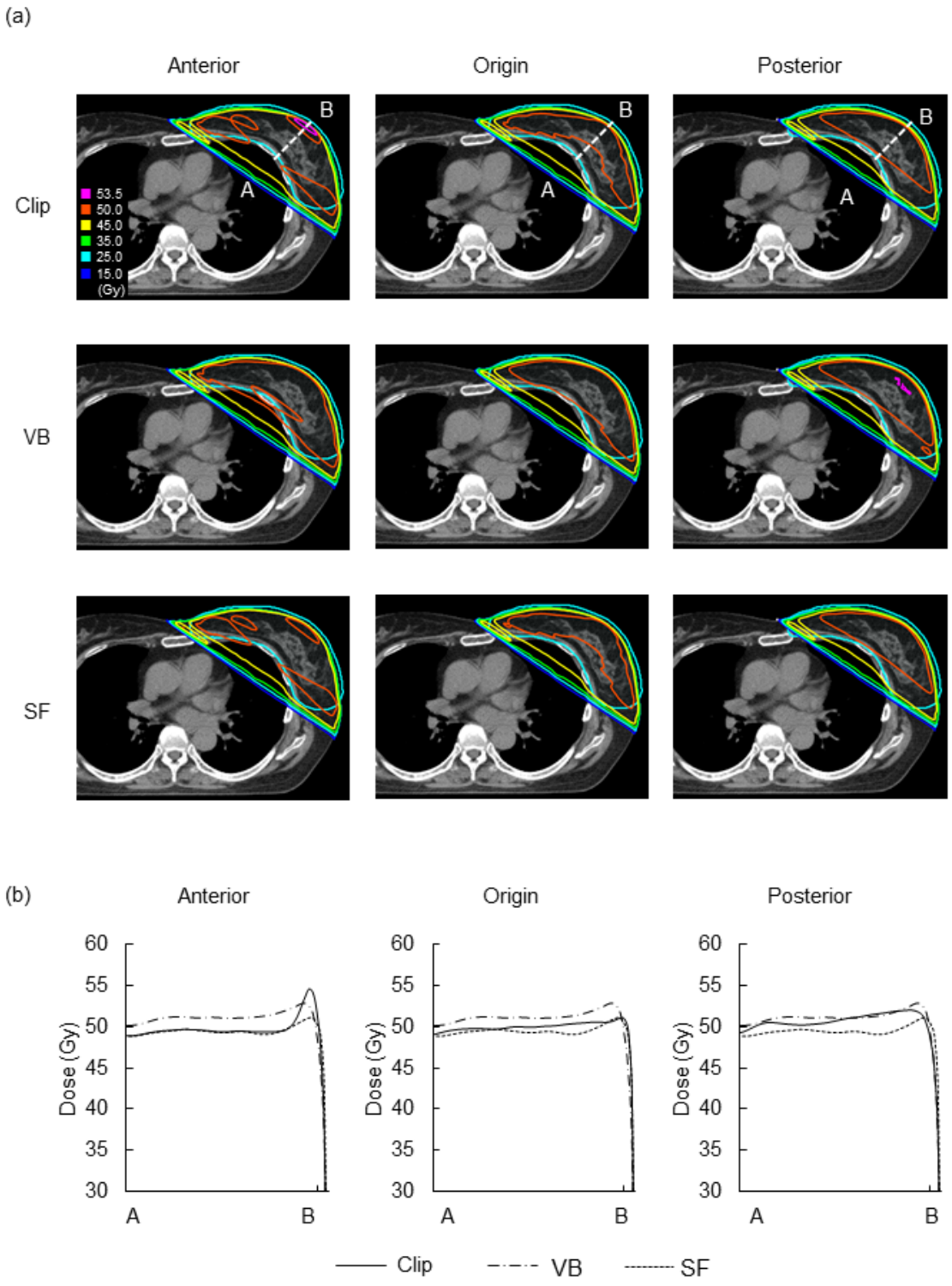

Figure 3

Dose distributions for plans used in direct mode

(a) From the left column, the following data are shown in direct mode: dose distribution after shifting in the anterior direction, the dose distribution at the origin position, and dose distribution after shifting in the posterior direction. Each row, from top to bottom, shows the clipping, virtual bolus, and skin flash plans. (b) Dose profile along line AB for plans after shifting in the anterior direction, at the origin position, and after shifting posterior direction

Abbreviations: VB; virtual bolus, SF; skin flash

Supplementary Files

This is a list of supplementary files associated with this preprint. Click to download.

- Tables.doc